Proceedings of the ASME/BATH 2021
Symposium on Fluid Power and Motion Control
FPMC2021
October 19-21, 2021, Virtual, Online

FPMC2021-68871

A POWER TAKE-OFF (PTO) FOR WAVE ENERGY CONVERTERS BASED ON THE HYBRID HYDRAULIC-ELECTRIC ARCHITECTURE (HHEA)

Jackson Wills
Dept. of Mechanical Engineering
University of Minnesota
Minneapolis, MN 55455
Email: wills224@umn.edu

Adam Keester *
Water Power Technologies Department
Sandia National Lab
Albuquerque, NM 87123
Email: akeeste@sandia.gov

Perry Y. Li †
Dept. of Mechanical Engineering
University of Minnesota
Minneapolis, MN 55455
Email: perry-li@umn.edu

ABSTRACT

Wave energy is a promising renewable energy resource for coastal regions around the world, but is not yet an economically competitive source of electricity. More effective power take-off (PTO) designs would help to make wave power a feasible and clean source of energy. To do this, PTOs need to: i) enable controlled actuation, ii) convert absorbed energy into electricity efficiently, and iii) have minimal manufacturing costs. We propose a new PTO architecture that can exert arbitrary control loads on the WEC to maximize energy capture, enabling the downsizing of expensive electrical components while maintaining high efficiency. Our PTO design is based upon a hybrid hydraulic-electric architecture (HHEA). This paper compares the performance of the HHEA PTO against two other PTO designs: 1) a baseline PTO consisting of a system of rectifying check valves and accumulators, and 2) a PTO consisting of an electro-hydraulic actuator (EHA). The HHEA PTO is shown to produce much more power than the check valve PTO and the EHA PTO. Also, the required electric generator sizes for the HHEA are smaller than that of the EHA PTO. The reduced size of these components allows for a WEC which is less expensive to manufacture.

1 Introduction

Wave energy represents an important opportunity for increased clean energy production as well as clean water production. It has the potential to generate massive amounts of energy [1] and has been studied to desalinate ocean water [2]. Wave energy is thus of particular interest because it may be able to aid humanity in such pressing issues as climate change and water scarcity, which are predicted to worsen dramatically in the coming years [3, 4]. The commercialization of this technology has been hampered by two main problems: the survivability of the device in extreme ocean weather is low, and the levelized cost of energy production from wave energy converters (WECs) is too high. The latter is due to the high monetary cost of manufacturing and upkeep compared to the amount of energy the device can produce. To address the second problem, it is important for each WEC to capture as much energy as possible and to transmit the captured power efficiently while keeping total cost low.

Fig. 1 illustrates the function of a power-takeoff (PTO) of converting the power from the WEC motion into electricity. The PTO can also play the role of controlling the WEC to operate in conditions that allow more energy to be captured from the waves. Many PTO strategies exist, including hydraulics, air turbines, hydro-turbines, as well as direct mechanical and electrical drives, [5]. Hydraulics are popular because of the high power involved. A review of hydraulic PTO designs can be found in [6].

Effective PTO architectures can help lower the levelized cost of energy (LCOE) of WECs. In order to do this, the PTO must be inexpensive and efficient in transmitting the captured energy

*Previously with the Department of Mechanical Engineering, University of Minnesota.

†Address all correspondence to this author.

to the generator. Also since effective control algorithms can dramatically increase the amount of energy capture [7], it is useful if the PTO can apply a controlled force on the WEC to execute motion that can capture the maximum energy.

This paper proposes a novel power take-off (PTO) design based upon the hybrid hydraulic-electric architecture (HHEA) as shown in Fig. 2. The HHEA was originally proposed for mobile machines in [8] to combine hydraulic actuation and electric actuation in a complementary manner. The majority of power is transmitted hydraulically via a set of common pressure rails and small electric components are only used to modulate this power to satisfy the requirement of the drive cycle. It has been shown to significantly reduce energy losses while keeping the electrical motor sizes at a fraction of what direct electrification requires [8, 9]. As a PTO for WECs, the potential advantages are power transmission efficiency, ability to control the WEC by exerting arbitrary forces, and the possibility to operate the main electric components at mean power instead of peak power. The latter is useful in reducing the electric component size and hence capital cost.

To understand the comparative attributes of the HHEA PTO, this paper presents a case study whereby the HHEA PTO is compared with two other hydraulic PTOs in the literature based on three main attributes. The other two PTOs are a rectifying check valve circuit that is efficient and inexpensive but lacks the ability to control the WEC arbitrarily, and one based on an electro-hydraulic actuator (EHA) which relies on the electric motor/generator to control the WEC. The three attributes to be considered are: i) the PTO's ability to control the motion of the WEC; ii) the PTO's ability to convert absorbed energy into electricity efficiently; and iii) the cost of the PTO. The end goal of these specifications is to lower the levelized cost of energy. The HHEA PTO is shown to be able to reduce the levelized cost of energy by downsizing electrical components while keeping power absorption high.

The rest of this paper is organized as follows. Section 2 presents the HHEA-PTO and the two other PTOs to be compared. The case study is presented in Section 3. Section 4 presents the results of the comparison. Section 5 presents concluding remarks.

2 Three Power Take-Offs for Comparison

The three hydraulic PTOs to be compared are presented in this section. Each PTO uses a hydraulic actuator mechanically connected to the WEC to first convert the mechanical energy of the WEC to hydraulic energy.

2.1 Hybrid Hydraulic-Electric Architecture

The hybrid hydraulic-electric architecture (HHEA) PTO is shown in Fig. 2. It consists of a set of common pressure rails

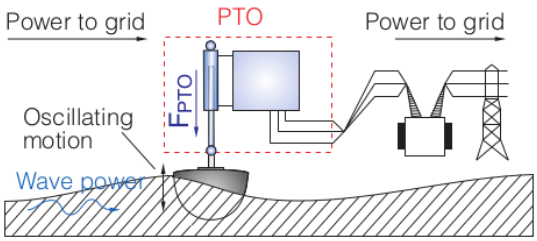

FIGURE 1: Definition of the power take-off (PTO) [10].

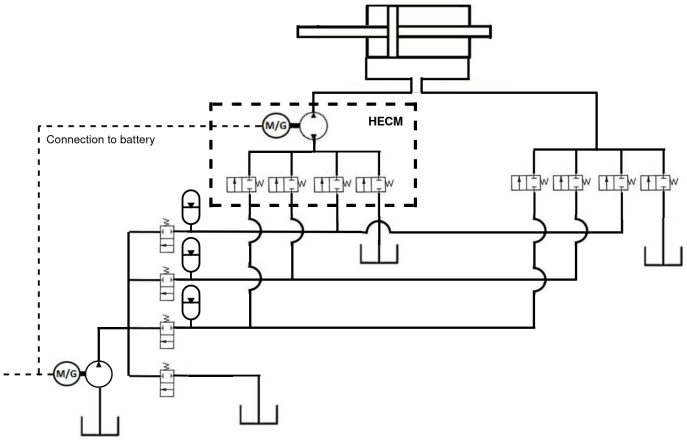

FIGURE 2: Simplified schematic of the HHEA system.

(CPRs) and a Hydraulic-Electric Control Module (HECM). The system can create any required output force by choosing a combination of hydraulic pressure rails and fine tuning the desired force electrically via the electric motor driven pump. Suppose there are n CPRs at pressure levels $p_{R1}, p_{R2}, \ldots, p_{Rn}$, the desired PTO force F_{PTO} can be met by a combination of pressure rail force $F_{rails}(p_A, p_B)$ and electric actuated force F_{elect}:

$$\underbrace{(P_A A_{cap} - P_B A_{rod})}_{F_{rails}(p_A,p_B)} + F_{elect} = F_{PTO} \tag{1}$$

where A_{cap} and A_{rod} are the cap and rod side areas of the actuator. In this case study, we consider a double ended actuator, so $A_{cap} = A_{rod}$. By choosing the CPRs, $p_A, p_B \in \{p_{R1}, p_{R2}, \ldots, p_{Rn}\}$, so that F_{rails} is close to F_{PTO}, the size of F_{elect} and hence the size and cost of the electric motor in the HECM can be reduced. As the n CPRs can provide potentially n^2 discrete F_{rails} levels, increasing n decreases the requirement for the HECM electric motor size, since the HECM need only provide half the difference between two adjacent rail forces. See Fig. 7 as an example.

The CPRs are fed by a fixed displacement pump/motor - electric motor/generator combination that is referred to as the

main motor/generator via a set of switching valves. The CPRs are assumed to have adequately sized accumulators for buffering flow so that the main motor/generator can be sized for mean power rather than peak power.

Notice that the HHEA is throttle-less by design and the switching valves are efficient in both the on and off states. The system can also utilize the hydraulic accumulators or electric battery to store and regenerate energy. It can also occasionally supply power to, instead of absorb power from, the WEC actuator.

The main differences between the HHEA-PTO and the HHEA proposed for mobile machines in [8] are that the direction of net power flow is opposite (the PTO absorbs net power from, instead of supplying power to, the WEC actuator), and that the electric motor/generator has replaced the role of the I.C. engine.

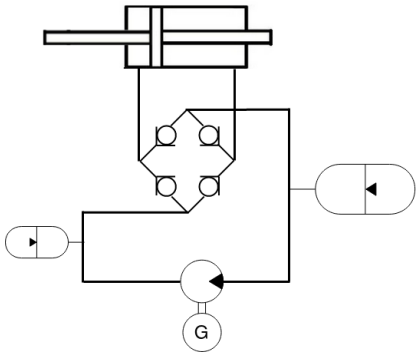

FIGURE 3: Schematic of the check valve PTO.

2.2 Check Valve PTO

The check valve PTO consists of a set of rectifying valves, two accumulators, a hydraulic motor and an electric generator (Fig. 3). As the piston moves, pressure builds and flow is directed to the high pressure accumulator by the rectifying valves. The rectifying valves ensure that high pressure fluid is directed to the high pressure accumulator regardless of whether the piston is extending or retracting. The presence of the accumulators ensures that the pressure across the hydraulic motor is nearly constant. The rotary generator is operated at a constant speed. Because of the constant pressure and speed, the motor and generator can be operated at near peak efficiency. However, the load acting on the WEC actuator is determined by the pressures in the accumulators, which cannot be varied quickly to provide arbitrary load on the actuator.

2.3 Electro-Hydrostatic Actuator PTO

The EHA PTO consists of a bidirectional, variable displacement hydraulic pump/motor and an electric generator (Fig. 4). The generator is operated at constant speed, and the fractional displacement of the hydraulic pump can be varied with time to achieve the desired drive cycle. Because the displacement of the pump is variable, the system is controllable. It is therefore expected that the EHA PTO will be able to execute the optimal control drive cycle.

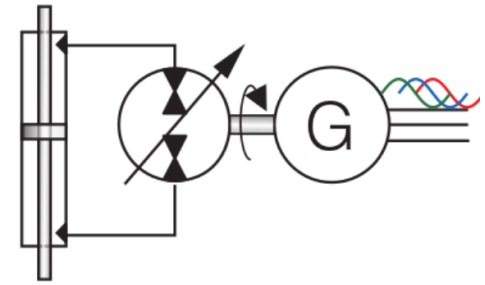

FIGURE 4: Schematic of the electro-hydrostatic actuator (EHA) PTO.

3 Case Study

3.1 OSWEC and WEC-Sim

The WEC device studied here is the oscillating flap or oscillating surge WEC (OSWEC) (Fig. 5). In the OSWEC archetype, a hinged flap rotates over a fixed or moored base, perpendicular to incoming waves. Many variations on the OSWEC have been developed, including the Oyster [11], the WaveRoller [12], the Langlee OSWEC [13], the Resolute Marine Energy OSWEC [14], or the Reference Model 5 (RM5) [15]. The OSWEC studied in this paper is the model in WEC-Sim's PTO-Sim application [16] and is bottom-fixed and approximately 11.5m tall and 18m wide. A schematic of a general OSWEC is shown in Fig. 5.

Due to the high cost of experimental ocean testing, the ability to test a WEC via computer simulation is extremely important. The Wave Energy Converter Simulator (WEC-Sim) is a tool developed by Sandia National Lab (SNL) and NREL [17] for this purpose. It is a MATLAB-Simulink-Simscape based program that simulates a WEC coupled with various controllers, PTOs, and moorings over a variety of sea states [17]. WEC-Sim has been validated for various WEC cases. Here, the PTO-Sim OSWEC model is analyzed using the WAMIT boundary element method hydrodynamic coefficients available in WEC-Sim.

The wave spectrum considered here is the regular wave spectrum with a height of 2.5 meters and a period of 8 seconds. The simulation is run in WEC-Sim for 200 seconds and allows for 50 seconds of ramp time for the WEC motion to move out of its start-up phase. No mooring system is considered; the WEC is considered fixed to the ocean surface. The device geometry,

mass and hydrodynamic coefficients are identical to the OSWEC device in WEC-Sim's PTO-Sim Application.

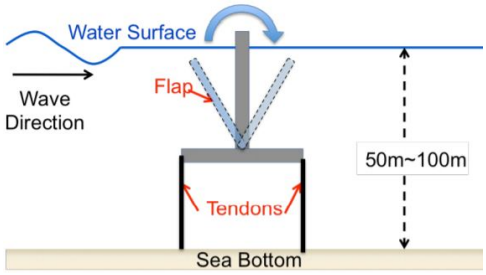

FIGURE 5: Schematic of a general OSWEC device. Reproduced from [15].

3.2 Control Method and Drive Cycle

The force F_{PTO} that the actuator exerts onto the WEC is important for controlling the WEC motion to maximize the power absorbed from the waves. It has been shown that control strategies play a key role in the amount of energy that can be captured. An non-exhaustive list of control strategies include [7, 18–20]. Instead of focusing on control strategy design, this paper is concerned with the PTO's ability to execute a desired drive cycle specified by the control law. The drive cycle consists of a motion and force on the actuator, $(x(t), F_{PTO})$.

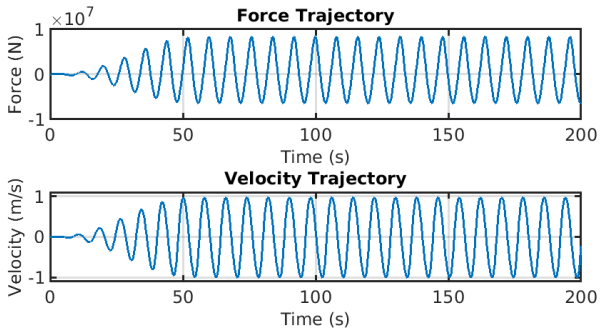

FIGURE 6: Force and velocity trajectories to be tracked by the PTOs.

Power is the multiplication of a force and a velocity. All power take-offs must balance between supplying a high enough resistive force to constrain a WEC and generate power with a low enough force to allow the WEC to move and respond to an incoming wave. If considering a linear system, the WEC control strategy that maximizes the energy capture is one that matches the impedance of the WEC. Since the linearized WEC dynamics in the Laplace domain are:

$$\underbrace{\left(s(M+m(\omega))+B_v+R(\omega)+\frac{S}{s}\right)}_{Z(s)}v(s)=F_e(s)+F_{PTO}(s) \tag{2}$$

where $v(s)$ is the WEC's velocity, M is the inertia of the WEC, $m(\omega)$ is the hydrodynamic added mass at the excitation frequency, $B_v+R(\omega)$ is the drag and radiative damping coefficient, S is the hydrostatic stiffness, $F_e(s)$ is the excitation force, and $F_{PTO}(s)$ is the PTO force, the feedback control that maximizes the energy capture is the conjugate of the impedence:

$$F_{PTO}(j\omega)=Z^*(j\omega)v(j\omega)=Z(-j\omega)v(j\omega) \tag{3}$$

When the excitation frequency ω is known, a proportional-integral controller can be used to determine the PTO force

$$F_{PTO}(s)=\frac{K_p s+K_i}{s}v(s) \tag{4}$$

in such a way that $K_p+\frac{K_i}{j\omega}=Z(-j\omega)$. Details of the derivation are in [21].

Since only regular waves are considered here, the PI control will be optimal. This is a significant simplification but this paper is only concerned with the PTO architecture's ability to realize a control law, and not the derivation or generality of that control law. Applying this PI controller to the OSWEC in WEC-Sim resulted in the drive cycle for the PTO force and WEC velocity trajectories $(F_{PTO}(t), v(t))$ as shown in Fig. 6. The force and velocity are out of phase, which means that the power is bidirectional.

For the HHEA-PTO and EHA-PTO, the drive cycle in Fig. 6 will be tracked. For the check-valve PTO, since the desired F_{PTO} cannot be achieved, the force the PTO enacts on the WEC is determined exclusively by the trajectory of the WEC as in [16].

3.3 PTO-Modeling

The subject of this paper is to compare each PTO on three specifications. First, can the PTO control the motion of the WEC? Second, how efficiently can the PTO convert absorbed energy into electricity? And third, how expensive is the PTO? While the first question can be answered by inspection of each PTO, the second and third questions require more analysis. To answer these questions, each PTO was modeled to calculate the efficiency and required component sizing of each PTO.

In all 3 PTOs, the working fluid is assumed to be incompressible. All electrical motor/generators were assumed to be 90% efficient. The efficiency characteristics of the hydraulic pump/motors used are taken from that of a bent-axis pump/motor in [22,23] with displacement scaled to the values appropriate for the PTOs. For the HHEA-PTO and EHA-PTO, static analysis are performed. The check-valve PTO is simulated in WEC-Sim where accumulator dynamics are accounted for (see [16]).

3.3.1 HHEA-PTO For the HHEA-PTO, the common pressure rails (CPRs) are assumed to always be at the prescribed pressure level. Line losses are ignored. The accumulators on the CPRs are assumed to be sufficiently large so that the power flow between the main motor-generator and each rail is unidirectional. Throttling losses are present during each switch from one CPR to another.

Throttling losses result from the following. Either end of the cylinder may be receiving flow from any one of the available CPRs at each time. If it is desired that the CPR connected to either end of the cylinder should switch to another CPR, then two things must happen. First, the valve that was previously open must be closed. Second, the valve corresponding to the desired CPR must be opened. Because there will be a pressure difference across, and a flow through, each valve as this happens, there will be energy lost. To minimize this loss, there is a small delay (15 ms) between the closing of the first valve and the opening of the second. The valve is modeled as a second order underdamped system. The valve is assumed to be able to close or open in 35 ms. These losses occur each time it is desired there be a switch of CPRs at either end of the cylinders. The amount of energy lost per switch depends on the velocity of the WEC at the time of the switch.

The selection of pressure rails over the course of the drive cycle was determined using an optimization algorithm modified from [24] that minimizes the energy losses:

$$\min_{d(\cdot)} \int_0^T Loss_{HECM}(t,d(t))dt + \sum_{i=1}^{n} Loss_{MG,i}(V_i) \qquad (5)$$

where $d(t)$ is the selection of the CPRs at each instance, $Loss_{HECM}(t,d(t))$ are the power losses in the electric generator/drive and hydraulic pump/motor with the HECM, and $Loss_{MG,i}$ is the losses in the main generator and hydraulic pump/motor associated with supplying or absorbing flow from each pressure rail i. Since this latter loss depends on the direction of the net flow V_i on each rail, the optimization algorithm in [24] decomposes the original optimization problem into multiple sub-problems to be solved. A major difference between here and the I.C. engine powered case considered in [24] is that the net battery use equality constraint is removed since the net power source/sink is the electric grid. Throttling losses are not included in the optimization done here but are added back when calculating energy captured. Future work is needed to include these losses in the optimization algorithm. Including them will only improve the performance of the HHEA PTO.

A hydraulic pump/motor is required to supply or absorb the net flow in each rail. The electric generator is operated at a constant speed of 3000 RPM. The rail selections chosen for this drive cycle result in only one rail having a non-zero net flow; and the accumulators are assumed to be large enough to handle swings in flow. Because of this, the main hydraulic pump/motor can operate at full displacement, and constant power to deal with the flow from that rail.

After the pressure rail choices are selected, the required torque from the HECM unit is known. The rotational velocity of the HECM is determined by the velocity of the WEC. With the required speed and torque, the maximum energy required to be processed by the HECM generator can be calculated. This determines the required size of the HECM generator. The size of the HECM pump/motor is determined exclusively by the velocity trajectory of the WEC.

3.3.2 Check Valve PTO The modeling and simulation of the check valve PTO are done using WEC-Sim [17, 25]. The check valve PTO is described in [16] and the reader is referred to this paper for more details. The electric generator is the same in all three PTOs. It is important to note that this PTO is not controllable, and therefore did not follow the same drive cycle force and velocity trajectories as the other two PTOs. This is an inherent disadvantage of the check valve PTO.

This model considers incompressiblity effects. Flow through the check valves are modeled using a modified orifice equation. Accumulator dynamic are modeled such that the pressure in each accumulator is dependent on the instantaneous volume of in each accumulator. For more details on the model, see [16].

3.3.3 EHA A static model is also used to model the electro-hydraulic actuator PTO. The electric generator and variable displacement hydraulic pump/motor are sized for the drive cycle as determined by the PI controller. The electric generator is assumed to operate at constant speed of 3000 RPM. The motor's displacement at each time instant is determined to achieve the desired force and velocity of drive cycle. Energy losses are then computed based upon the component efficiency characteristics.

4 Results

4.1 Hybrid Hydraulic-Electric Architecture PTO

The pressure rail force selection (by selecting pair of CPRs) is shown in Fig. 7. The optimal spacing of the four pressure rails

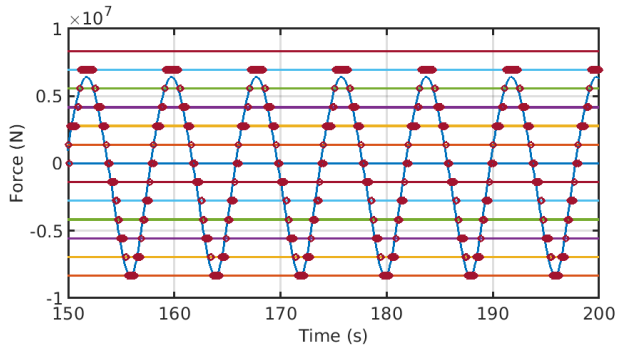

FIGURE 7: Rail force options are shown along with the desired force trajectory. The red circles denote which pressure force was selected at each time. The difference between the pressure force selected and the desired rail force is made up by the HECM motor. Top: three pressure rail architecture. Bottom: four pressure rails architecture.

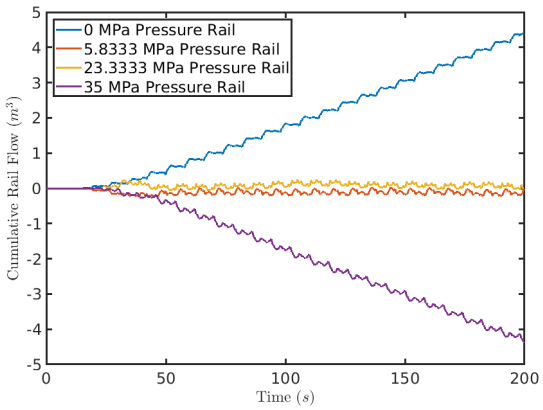

FIGURE 8: Cumulative flow in each pressure rail. Positive flow is flow out of the accumulator, towards the actuator.

is not uniform. Thus, since the actuator areas are equal, there are 13 distinct rail forces. Note that the algorithm picks the rail force either above or below the drive cycle force. This ensures that pressure rails supply most of the energy required to achieve the drive cycle with the HECM making up the difference to achieve the desired trajectory.

When a pressure rail is selected, there may be flow into or out of that rail's accumulator depending on the velocity of the WEC. The flows in each rail are shown in Fig. 8. If the accumulators are large enough, then the main pump need only tap flow from the 35 MPa rail.

The power buffering quality of the HHEA PTOs can be seen in Fig. 9. The main motor is able to operate at a constant power. The HECM however, must adjust its power output as the drive cycle changes. The angular speed of the HECM unit is dictated by the velocity trajectory of the WEC, while the torque of the HECM is dictated by the desired force trajectory and the choice of rail force.

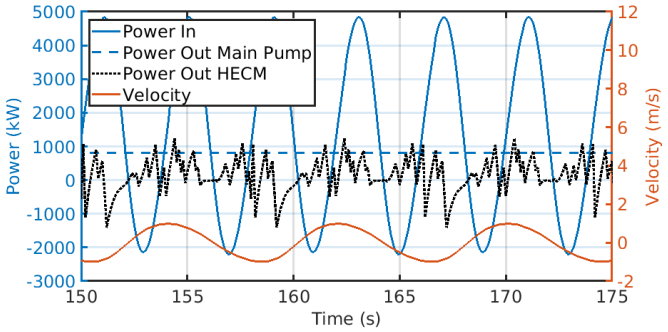

FIGURE 9: Results for the HHEA PTO. Power into the system (PTO force times velocity) is shown. The velocity shown is the velocity of the hydraulic piston over time. Electricity is produced at both the main pump and the HECM.

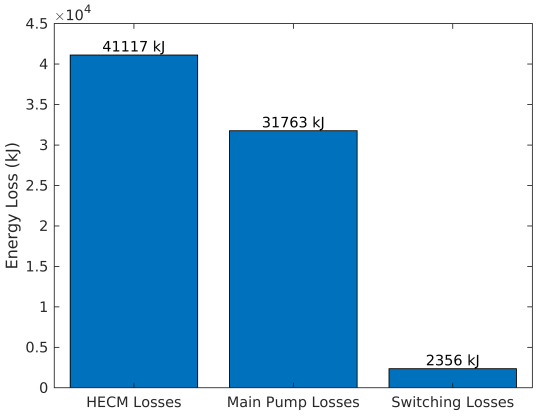

FIGURE 10: Breakdown of losses in the HHEA PTO.

Fig. 10 compares the sources of losses in the HHEA PTO. Main pump and HECM losses are due to inefficiencies in their hydraulic pump/motor and electric motor/generators. Switching losses result from the dynamics involved in switching between the CPRs.

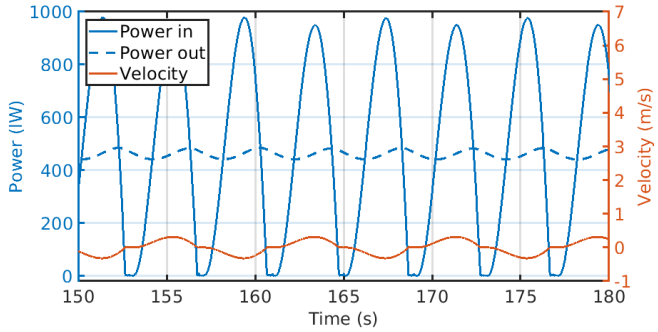

FIGURE 11: Power in and out of the check valve PTO over time. The velocity shown is the velocity of the hydraulic piston over time.

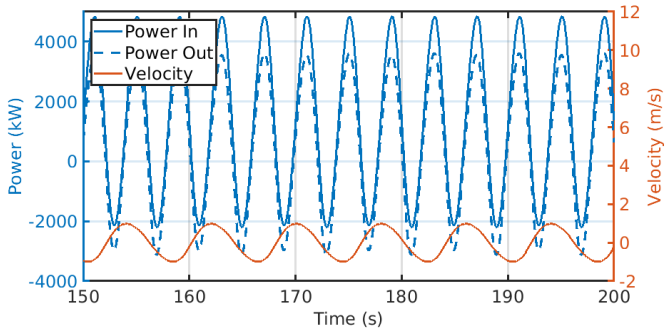

FIGURE 13: Power in and out of the EHA PTO over time. The velocity shown is the velocity of the hydraulic piston over time.

4.2 Check Valve PTO

Power absorption over time is shown for the check valve PTO in Fig. 11. Notably, the power out does not fluctuate very much as the power in does. The power out remains around the mean of the power in. This quality is called power buffering, and allows for electrical components to be sized closer to the mean than the peak of the power in. The total efficiency was found to be 86%, the highest of all PTOs compared here. The check valve PTO absorbs significantly less power than the other PTOs due to its inability to realize the optimal force trajectory. This reduced power absorption is the main weakness of this PTO and can be seen clearly in Fig. 14. While the check valve PTO has many strengths (power buffering, small electrical components, high efficiency) it is not a competitive PTO because the force it enacts on the WEC cannot be controlled and thus its power absorption is dwarfed by other PTO designs. It is a cheap and efficient PTO but it has a high LCOE because it produces such little energy.

4.3 Electro-Hydrostatic Actuator PTO

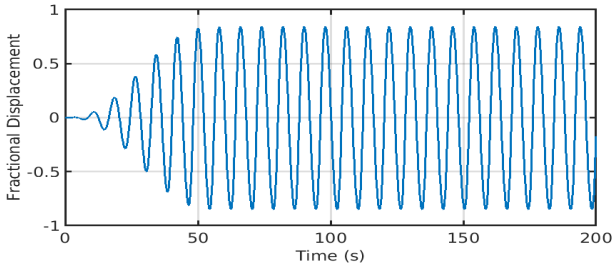

FIGURE 12: Fractional displacement of the bidirectional variable displacement motor for the EHA PTO.

The EHA PTO is perhaps the most straight forward way to arbitrarily control a WEC using a hydraulic PTO. The displacement of the pump/motor is varied to achieve the drive cycle. The required fractional displacement required to achieve this particular drive cycle is shown in Fig. 12. The power generated by the EHA PTO is in phase with the power absorbed by the WEC (Fig. 13). The difference between the power in and power out are due to inefficiencies in the pump motor and the generator. The notable take-aways from the EHA results are that the EHA PTO is able to absorb large amounts of energy (because the force can be controlled) but the power is not smoothed in any way. This is a problem if the power is bidirectional, as it is here. It also means that the electrical components need to be sized for the peak power and will therefore be expensive.

4.4 Comparison between the 3 PTOs

The cumulative power captured from each PTO are shown in Fig. 14 and 15. Fig. 15 shows the average electrical power production from each PTO during the final 100 seconds of the simulation (well after the start up-phase, the behavior in this time period is assumed to continue indefinitely). The HHEA produces the most power/energy, followed by the check valve PTO and the EHA PTO which produce similar amounts. This is somewhat surprising because the EHA is able to realize the optimal controller, and thus has more than double the energy input than the check valve PTO.

Fig. 16 shows that the check valve PTO is the most efficient, followed by the HHEA PTO, and the EHA PTO is the least efficient which explains why the EHA PTO does not produce as much energy as expected.

To understand this, the operating points of the EHA pump/motor for this drive cycle are overlaid over its efficiency contours in Fig. 17. The pump/motor operates in all 4 quadrants so that power goes in both directions from hydraulics to electric and vice versa. There are also many instances where the pump/motor is operated at low efficiencies. Define the mean in-

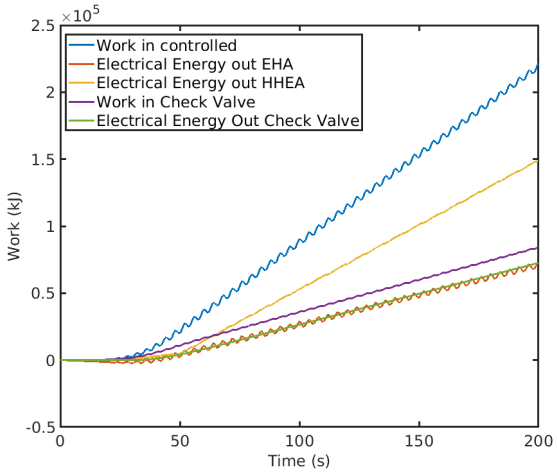

FIGURE 14: The amount of energy absorbed (work in) is shown along with the amount of energy converted into electricity by each PTO (work out).

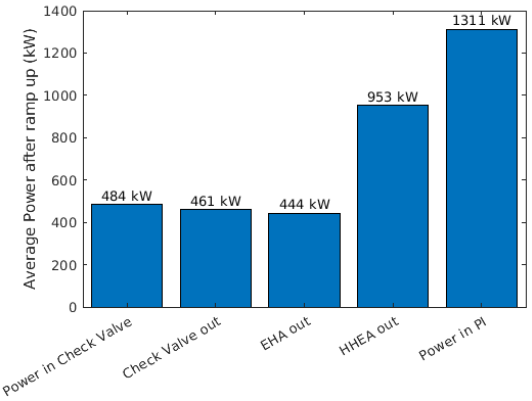

FIGURE 15: Average electrical power output over the last 100 seconds. This time period was chosen so that no transient effects from ramp up are included.

stantaneous efficiency as:

$$\bar{\eta} := \frac{W_{hydraulic,out} + W_{electric,out}}{W_{electric,in} + W_{hydraulic,in}} \tag{6}$$

where $W_{hydraulic,in}$ and $W_{electric,in}$ are respectively the total work inputs when the hydraulic power or the electric power are acting positively on the EHA; and similarly, $W_{hydraulic,out}$ and $W_{electric,out}$ are respectively the total work outputs when the EHA is acting positively on the WEC or on the electric generator. All W_* are defined to be positive. The mean instantaneous efficiency

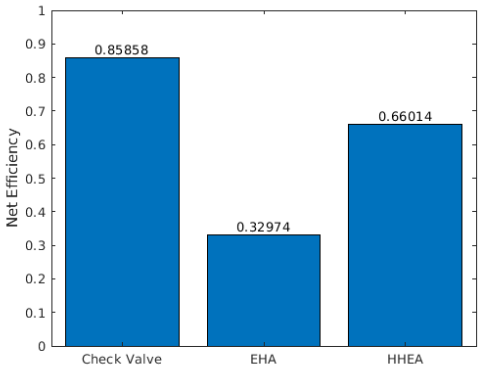

FIGURE 16: Comparison of the net efficiency of each PTO. Efficiency is defined as the final amount of power absorbed over the final amount of energy converted into electricity.

of the EHA PTO is 67%.

With such a high mean instantaneous efficiency, why is the net efficiency of the EHA PTO only 33%? The reason lies in the bidirectional nature of the incoming power (see Fig. 13). For every 7 positive units of work ($W_{hydraulic,in}$), there are roughly 2 units of negative work ($W_{hydraulic,out}$), leaving a net work of $7-2=5$ units. The EHA PTO gets taxed twice so to speak. Assume that the instantaneous efficiency is constant at 67%. While capturing the 7 units of positive input, the system outputs 4.7 units of electrical work. When the system needs to produce the 2 units of negative work, 3.0 units of electrical energy is consumed. Thus the system has converted a net $4.7-3.0=1.7$ units of electrical work. The system's net efficiency is $1.7/5=34\%$, which is very similar to the observed net EHA PTO efficiency of 33%.

The EHA is hindered by the bidirectionally of the incoming power, and by low efficiency operating points. The HHEA, on the other hand, is largely able to skirt these problems. One main advantage of the HHEA PTO is that most of the power is obtained from the main pump/motor, not the HECM (see Fig. 9). The accumulators allow energy to be stored in the form of pressurized fluid. The main pump/motor can then empty or fill these accumulators steadily. The main pump/motor is able to operate at constant torque and speed, thus generating a constant power at high efficiency. The HECM does have to vary its operating points and provide both positive and negative flow. It has roughly 7 units of positive power to every 3 units of negative power. The main pump, on the other hand, only provides positive power as the accumulator is able to store and recycle energy. Taken together, the HECM and main pump collect about 8 units of positive power for every 1 unit of negative power. Indeed the net efficiency of the HECM is also low and as shown in Fig. 10, the HECM does account for the majority of the losses. Still, since it is responsible for a smaller fraction of the power than the main

pump, the overall effect of the power cycling within the HECM is reduced.

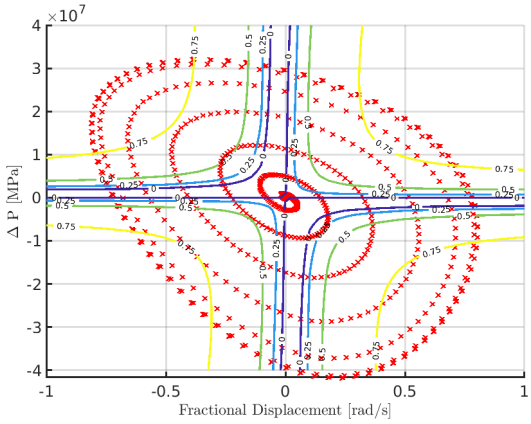

FIGURE 17: The efficiency map of the pump/motor in the EHA PTO. The red x's show operating points used in this drive cycle.

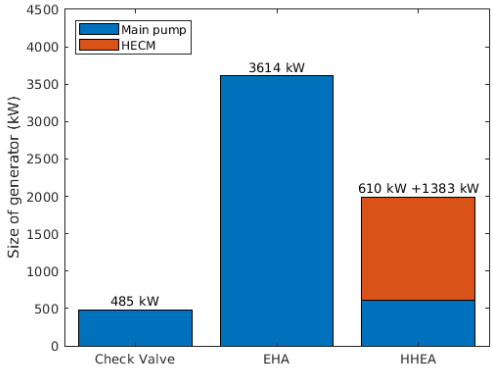

FIGURE 18: The required size of all generators. The maximum power supplied to or received from the generator determines its required size.

Required component sizes are compared in Figs. 18 and 19. The check valve PTO requires the smallest generator because its output power is small. The HHEA PTO requires two generators, but the total power is still smaller than that required by the EHA PTO. One the other hand, the HHEA PTO requires one large hydraulic pump/motor and one small hydraulic pump/motor. The large pump/motor required by the HHEA is the HECM pump/motor. It is sized by the maximum drive cycle velocity and the actuator area. Thus it would have the same size as

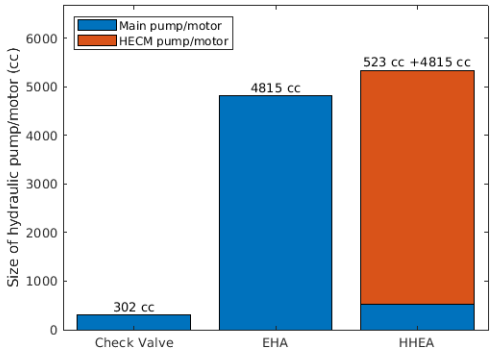

FIGURE 19: The required size of all pumps and motors. The maximum flow rate through the pump or motor determines its required size.

the EHA pump/motor but has a lower pressure requirement. The main pump/motor of the HHEA is required to deal with non-zero net flow in the pressure rails (see Fig. 8). On whole, the HHEA PTO shows good performance on energy production, controllability and requirement for small electrical components.

5 Conclusions

A novel hybrid hydraulic electric architecture (HHEA) power take-off (PTO) design was proposed with the potential to reduce the levelized cost of energy (LCOE). This is possible because the common pressure rails absorb most of the energy, while the hydraulic electric control module (HECM) is responsible only for the small amount of remaining energy needed to realize the optimal control strategy. Thus, the HHEA PTO can produce a competitive amount of energy while lowering the required size of expensive electric generators.

The HHEA PTO was compared to two other PTO designs. We set out to compare these PTOs on three attributes: i) the PTO's ability to control the motion of the WEC; ii) the PTO's ability to convert absorbed energy into electricity efficiently; and iii) the cost of the PTO. The end goal of these specifications was to lower the levelized cost of energy. The HHEA and EHA PTOs succeed in controlling the motion of the WEC, while the check valve PTO fails. Both the check valve and HHEA PTOs were able to convert absorbed energy into electricity with high efficiency. Lastly, the HHEA and check valve PTOs require smaller electric generators (hence, likely cost) than EHA PTO. The HHEA PTO was able to output roughly double the electrical power than the EHA and check valve PTOs. The HHEA does require about 4 times larger generators than the check valve PTO, but its generators are about half the size required by the EHA.

Future work includes analyzing irregular wave spectra. The HHEA design and modeling could also be improved. One or

more transformers could be added to produce the middle pressure rails. The rail selection algorithm could be augmented to include switching losses, and an algorithm for how and when the main pump should provide flow to each rail could be developed. Additionally, a different scheme for refilling and removing flow from the CPRs may be able to reduce the main hydraulic and electric component sizing.

REFERENCES

[1] Garanovic, A., 2021. NREL publishes marine energy resource report for united states, Feb.

[2] Hicks, D., Pleass, C., and Mitcheson, G., 1988. "Delbuoy: wave-powered seawater desalination system". *OCEANS 88. A Partnership of Marine Interests. Proceedings*.

[3] OECD, 2015. *The Economic Consequences of Climate Change*. OECD Publishers, Paris. https://doi.org/10.1787/9789264235410-en.

[4] Boretti, A., and Rosa, L., 2019. "Reassessing the projections of the world water development report". *npj Clean Water,* **2**(1).

[5] Têtu, A., 2019. *Handbook of ocean wave energy*. SPRINGER.

[6] Jusoh, M. A., Ibrahim, M. Z., Daud, M. Z., Albani, A., and Mohd Yusop, Z., 2019. "Hydraulic power take-off concepts for wave energy conversion system: A review". *Energies,* **12**(23).

[7] John, J., Bacelli, G., and Fusco, F., 2014. "Energy-maximizing control of wave-energy converters: The development of control system technology to optimize their operation". *IEEE Control Systems,* **34**(5), p. 30–55.

[8] Li, P. Y., Siefert, J., and Bigelow, D., 2019. "A hybrid hydraulic-electric architecture (hhea) for high power off-road mobile machines". *ASME/BATH 2019 Symposium on Fluid Power and Motion Control*.

[9] Siefert, J., and Li, P. Y., 2020. "Optimal control and energy-saving analysis of common pressure rail architectures: HHEA and STEAM". In BATH/ASME 2020 Symposium on Fluid Power and Motion Control, American Society of Mechanical Engineers Digital Collection.

[10] Hansen, R. H., 2013. "Design and control of the powertake-off system for a wave energy converter with multiple absorbers". PhD thesis, Department of Energy Technology, Aalborg University.

[11] Whittaker, T., and Folley, M., 2012. "Nearshore oscillating wave surge converters and the development of oyster". *Philosophical Transactions of the Royal Society,* **370**, pp. 345–364.

[12] Lucas, J., Livingstone, M., Vuorinen, M., and Cruz, J., 2012. "Development of a wave energy converter (wec) design tool – application to the waveroller wec including validation of numerical estimates". In 4th International Conference on Ocean Energy.

[13] Pecher, A., Kofoed, J., Espedal, J., and Hagberg, S., 2010. "Results of an experimental study of the langlee wave energy converter". In 20th International Offshore and Polar Engineering Conference, Langlee Wave Power.

[14] Ramudu, E., 2011. "Ocean wave energy-driven desalination systems for off-grid coastal communities in developing countries". In 2011 IEEE Global Humanitarian Technology Conference, Resolute Marine Energy.

[15] Yu, Y., Jenne, D., Thresher, R., Copping, A., Geerlofs, S., and Hanna, L., 2015. Reference model 5 (rm5): Oscillating surge wave energy converter. Technical Report NREL/TP-5000-62861, NREL, January.

[16] So, R., Simmons, A., Brekken, T., Ruehl, K., and Michelen, C., 2015. "Development of pto-sim: A power performance module for the open-souse wave energy converter code wec-sim". In In Proceedings of OMAE 2015.

[17] Yu, Y., Lawson, M., Ruehl, K., and Michelen, C., 2014. Development and demonstration of the wec-sim wave energy converter simulation tool. Technical Report SNL2014-3013C, SNL.

[18] Nie, R., Scruggs, J., Chertok, A., Clabby, D., Previsic, M., and Karthikeyan, A., 2016. "Optimal causal control of wave energy converters in stochastic waves – accommodating nonlinear dynamic and loss models". *International Journal of Marine Energy,* **15**, p. 41–55.

[19] Li, G., Weiss, G., Mueller, M., Townley, S., and Belmont, M. R., 2012. "Wave energy converter control by wave prediction and dynamic programming". *Renewable Energy,* **48**, Jun, p. 392–403.

[20] Scruggs, J., Lattanzio, S., Taflanidis, A., and Cassidy, I., 2013. "Optimal causal control of a wave energy converter in a random sea". *Applied Ocean Research,* **42**, p. 1–15.

[21] Coe, R., Bacelli, G., Nevarez, V., Cho, H., and Wilches-Bernal, F., 2018. A comparative study on wave prediction for wecs. Technical Report SAND2018-10945, SNL.

[22] Pourmovahed, A., Beachley, N. H., and Fronczak, F. J., 1992. "Modeling of a hydraulic energy regeneration system: Part l—analytical treatment". *Journal of Dynamic Systems, Measurement, and Control,* **114**(1), p. 155–159.

[23] Pourmovahed, A., Beachley, N. H., and Fronczak, F. J., 1992. "Modeling of a hydraulic energy regeneration system: Part ll—experimental program". *Journal of Dynamic Systems, Measurement, and Control,* **114**(1), p. 160–165.

[24] Siefert, J., and Li, P. Y., 2020. "Optimal operation of a hybrid hydraulic electric architecture (hhea) for off-road vehicles over discrete operating decisions". *2020 American Control Conference (ACC)*.

[25] Yu, Y.-H., Ruehl, K., Rij, J. V., Tom, N., Forbush, D., Ogden, D., Keester, A., and Leon, J., 2020. Wec-sim v4.2. Tech. rep., December.